A Micromachined Electron Source

D.A. Crewe, D.C Perng, S.E. Shoaf, and A.D. Feinerman
University Of Illinois at Chicago
Microfabrication Applications Laboratory
Chicago, Illinois, 60680

Abstract

A new microfabrication technique that allows the precise construction of large three dimensional structures with dimensional tolerances approaching 1 micron is being applied to the design of a Miniature Scanning Electron Microscope (MSEM). In this paper we will present the electron optic calculations of the MSEM source (gun). The MSEM measures less than one cubic centimeter and the source measures approximately $1\times1\times0.20$ cm^3 . The details of the MSEM fabrication are in an accompanying article.[1]

There are many advantages of a MSEM. The performance of an SEM is improved as its length is reduced.[2] The need for mechanical adjustments and motion feedthroughs is eliminated since the microscope components are pre-aligned to the optic axis. All components are ultra high vacuum compatible and can be heated to 500 °C. A small, portable electron microscope can be brought to the sample to be inspected instead of the sample being brought to the microscope. Vacuum hardware requirements are minimized. The fabrication technology is inexpensive with respect to the conventional methods of electron microscope construction. Arrays of MSEMs can be built to allow applications in high throughput e-beam lithography. In addition two MSEMs can be mounted a few degrees apart to provide stereo imaging.

1. Electron Optic Calculations

1.1 Electrostatic Field Calculation

A three electrode design is preferred since it offers more control over magnification and beam crossover as other parameters in the MSEM lens system are developed. Three possible electrode arrangements that can be made using our construction method are shown in figure 1. The three element electrostatic lens is laid out on a rectangular mesh of 30,000 points. The density of mesh points along each direction can be varied, and more points are placed in regions where large spatial deviations in the electric field are expected. A finite difference solution to LaPlace's equation is then obtained using initial boundary conditions described by the grid. The electrodes are fixed potential surfaces and planes of parallel or normal field components can be assigned where appropriate. One can take advantage of symmetry in the lens by calculating one half the lens and mirroring the result about the optic axis.

0-8194-0950-2/92/$4.00

1.2 Ray Tracing and Optimum Lens Design

The potential on the optic axis is extracted from the finite difference solution and is the input to a fourth order Runga-Kutta paraxial ray trace routine that solves the equations of motion for electrons in the lens field with a given initial position and angle.

The various parameters that we are free to alter in the physical structure of the lens - the electrode thickness, electrode spacing, aperture sizes, and diaphragm thickness are adjusted until the resultant ray traces yield a well behaved lens. Once the physical layout of the lens is fixed the finite difference solution is obtained for a normalized potential on each of the electrodes. Three solutions are calculated for the three element lens, one for each of the electrodes at 1 kV and the other two at ground (fig. 2(a)). Using these three axial potentials one can obtain an axial potential distribution for an arbitrary assignment of electrode voltages by a scaled superposition (fig. 2(b)). If the first, second and third electrode potentials are V_1 V_2 and V_3 and the normalized axial potential for the three electrodes are $\phi_1(x)$, $\phi_2(x)$, and $\phi_3(x)$ then the total axial distribution is given by

$$\phi(x) = V_1\phi_1(x) + V_2\phi_2(x) + V_3\phi_3(x) \qquad (1)$$

Using this method the numerically intensive calculation of the electrostatic finite difference solution is employed only when the physical structure of the lens is changed. If the only change being made to the lens are the electrode potentials, equation (1) will give the axial potential distribution.

Desirable first order focal properties are a lens that can be focused in the range from infinity to points near the exit aperture of the gun with focussing potentials that do not change sign and are allowed by the insulating gap between the electrodes. An upper limit of 10 kv/mm is being adhered to in this design. The second lens figure 1 that has the focusing electrode aperture on the trailing edge of the die will focus at infinity with a second electrode potential of 250 volts (with the first and third electrode potentials at 1000 volts) and will focus at the final aperture with a potential of 50 volts. The focus position then is a strong, but controllable function of the second electrode potential. The first lens in figure 1 has the focusing aperture on the leading edge of the die and showed a stronger dependence on the focusing potential, requiring 170 volts and 40 volts for a focus at infinity and the gun exit, respectively. The third lens required a much higher potential difference to achieve the stronger focusing action since the gun exit aperture is closer to the source. For these reasons we settled on the general design of the second lens type, with the focusing electrode aperture on the trailing edge of the die.

1.3 Expected Performance

Minimization of the aberration coefficients is a primary lens design goal. Once a lens with good first order properties is obtained the task is to isolate those lens properties that contribute to large aberration coefficients and optimize the design to reduce their effect.

1.3.1 Spherical Aberration

Spherical aberration stems from the fact that electrons of different initial angles will focus to different radial positions in the image plane. The value of C_s at the *image* plane can then be calculated by tracing two rays with different initial angles and comparing the difference in their radial positions in the image plane. Assuming the ray is a straight line at the end of the trace - a reasonable assumption for focus positions outside the region of lens where the field is constant, the difference in radial position at the end of the trace Δr is related to the spherical aberration coefficient by

$$\delta_S = \Delta r_{C_s} = C_S(\Delta\alpha)^3 \tag{2}$$

Where α is the final angle of the converging beam, determined by apertures in the lens system. Spherical aberration can also be calculated directly by integrating over the output of a single ray trace using the following relation

$$C_S = \frac{1}{16\sqrt{V_3}} \int_o^i \left\{ \left[\frac{5}{4}\left(\frac{V''}{V}\right)^2 + \frac{5}{24}\left(\frac{V'}{V}\right)^4 \right] r^4 + \frac{14}{3}\left(\frac{V'}{V}\right)^3 r' r^3 - \frac{3}{2}\left(\frac{V'}{V}\right)^2 r'^2 r^2 \right\} \sqrt{V}\, dz \tag{3}$$

where r and r' are the radius and slope of the traced ray, respectively, at each point along the axis. V is the potential on the axis, V' and V'' are the first and second derivatives of the axial potential. V_3 is the potential on the third electrode. The integral is from the object plane to the image plane.[4]

1.3.2 Chromatic Aberration

Chromatic aberration stems from the existence of electrons with slightly different energy being focused by the field to different points in the image plane. The Chromatic aberration coefficient at the *image* plane can then be calculated by tracing two rays of different energies through the lens and comparing the difference in radial position of the focus

$$\delta_C = \Delta r_{C_c} = \frac{\Delta V}{V} C_C \alpha \tag{4}$$

Where ΔV is the difference in the two rays' energies. The chromatic aberration coefficient can also be calculated directly from a single ray trace by the following relation:[4]

$$C_C = \sqrt{V_3} \int_0^i \left(\frac{V'}{2Vr'} + \frac{V''r}{4V} \right) \frac{r}{\sqrt{V}} dz \tag{5}$$

From Equations 3 and 5 one can see that the aberration coefficients increase with fast spatial changes in V and V', corresponding to a rapidly varying electrostatic field. The optimal lens design therefore has a minimum of large field gradients. Lens B in figure 1 has a more gradual focussing effect due to the placement of the diaphragm containing the aperture on the trailing edge of the die (fig.3). One obvious point of field gradient is the thickness of the diaphragm containing the aperture. By increasing the thickness of the diaphragm from 30 to 225 microns (or roughly one half the 380 micron wafer thickness) the coefficient of spherical aberration at the image plane for a focus at the final aperture was reduced from 7.7 cm to 1.75 cm., beyond 225 micron diaphragm thickness the spherical aberration coefficient begins to increase. The Chromatic aberration coefficient improvement was not as dramatic, however (fig. 4). Thick diaphragms can be simulated with a structure like that shown in figure 5 in which two die are bonded together with zero gap between them to create one electrode. The large gap electrode to electrode alignment and bonding would be done in the same way as the simpler lens design. This electrode structure, while being much more difficult to build, shows the best theoretical performance.

1.4 Resolution

The resolution of the system can be calculated by plotting the effect of chromatic aberration in terms of the energy spread of the source and the final angle:

$$\delta_C = C_C \alpha \frac{\Delta V}{V} \tag{6}$$

Where α is in radians, δ and C_C are in Angstroms. A similar expression for spherical aberration:

$$\delta_S = 0.15 C_S \alpha^3 \tag{7}$$

And diffraction

$$\delta_d = \frac{0.61\lambda}{\alpha} = \frac{0.61 \times 12.3}{\alpha \sqrt{V}} \tag{8}$$

Where the wavelength λ is in angstroms and the potential in volts. These three expressions on the same plot versus the final angle of convergence are shown in figure 6 for two of the second

lens type in figure 1 at 1 kV beam potential with a focus position that corresponds to a working distance of 0.5 mm (the distance from the sample to the last defelction electrode). The intersection of the larger of the two aberration coefficients with the diffraction limit will give the smallest probe size and the size of the optimum aperture for the system. This type of plot will also show whether one of the aberration coefficients is dominating over the other. In this case we seem to be chromatic aberration limited. The improvement from the thin (8 μm) diaphragm lens design to the thick (225 μm) diaphragm is readily apparent from the plots, but since we are chromatic limited the dramatic improvement we saw in C_s isn't playing much of a role in the final performance of the lens. The effective probe size with thick diaphragms electrodes is 60 angstroms and with thin diaphragms is 70 angstroms. This probe size, when multiplied by the virtual source size and the magnification of the lens will give the expected resolution.

The magnification of our probe forming lens is defined to be

$$M = \frac{\alpha_i}{\alpha_o}\sqrt{\frac{V_i}{V_o}} \tag{9}$$

In our case the magnification is in the range 0.3-1.2 depending on the acceleration voltage used and the position of the focus.

With a cold field emission source having a virtual source size of 10 Angstroms, an energy spread of 0.1 eV, and a magnification of M=0.3, the thick diaphragm lens design will have a resolution of 180 angstroms, the thin diaphragm lens design 210 angstroms. It is unclear at this point whether or not this improvement in performance warrants the effort required to construct electrodes like those in figure 5.

2. Experimental Results

A four stack of electrodes consisting of a micromachined thermionic source and a three element electrostatic lens has been tested. The stack was attached to an AirPax© 18 pin glass sealed header that has been sealed into an ISO 2" quick flange and mounted to a vacuum system above a Faraday cup. The gun was run at a total emission current of 1 nA and a probe current of 20 pA and tested for focusing by changing the second electrode voltage and comparing the total and probe currents as more of the beam vignetted on the final aperture with a longer crossover. Thermionic sources, both macroscopic and microscopic are being used in the early development of the MSEM simply for convenience.

3. Conclusion

A new method of precisely aligning and bonding silicon die permits us to build a miniature scanning electron microscope with all it's components pre-aligned to the optical axis with a precision approaching one micron. Electron optic calculations were performed to arrive on an

optimum lens design for a simple probe forming system consisting of a three element electrostatic einzel lens and an electrostatic deflector system. The size of this simple MSEM is 1 x 1 x .28 cm^3. More complex MSEM design using the three element lens as a source and multiple lenses are being investigated. More complex systems involving the used of this source with a cold field emitter and a combination of magnetic lenses are being investigated.

4. Acknowledgements

This research is supported by NSF RIA 9009842 "Microfabrication of Electron Optical Components", a State of Illinois Challenge Grant "Microfabrication Applications Laboratory", and Monolithic Sensors Inc. "Stacking Of Pressure Transducers". The authors wish to Dr. Stanley Humphries of Acceleration Consultants and the University of New Mexico for advice on the use of the EMP 2.0 software which was used to perform the electrostatic field calculations, Dr. Peter Loeppert and James Branthaver of Monolithic Sensors for their help with silicon processing, and Prof. A.V. Crewe of the University Of Chicago for electron optics design suggestions.

6. References

1. A.D. Feinerman et. al., SPIE Optical Engineering Midwest, March 19, 1992
2. T.H.P. Chang, D.P. Kern, and D.P. Murray, J. Vac Sci Technol B, 8, 1698 (1990)
3. A.D Feinerman, S.E. Shoaf, and D.A. Crewe, "Precision Stacking and Aligning of Silicon Die" Proceedings, 180th Annual ECS Conference, Phoenix, AZ October, 1991
4. E. Munro, "A Set Of Computer Programs For Calculating the Properties Of Electron Lenses". University of Cambridge, England, 1978.

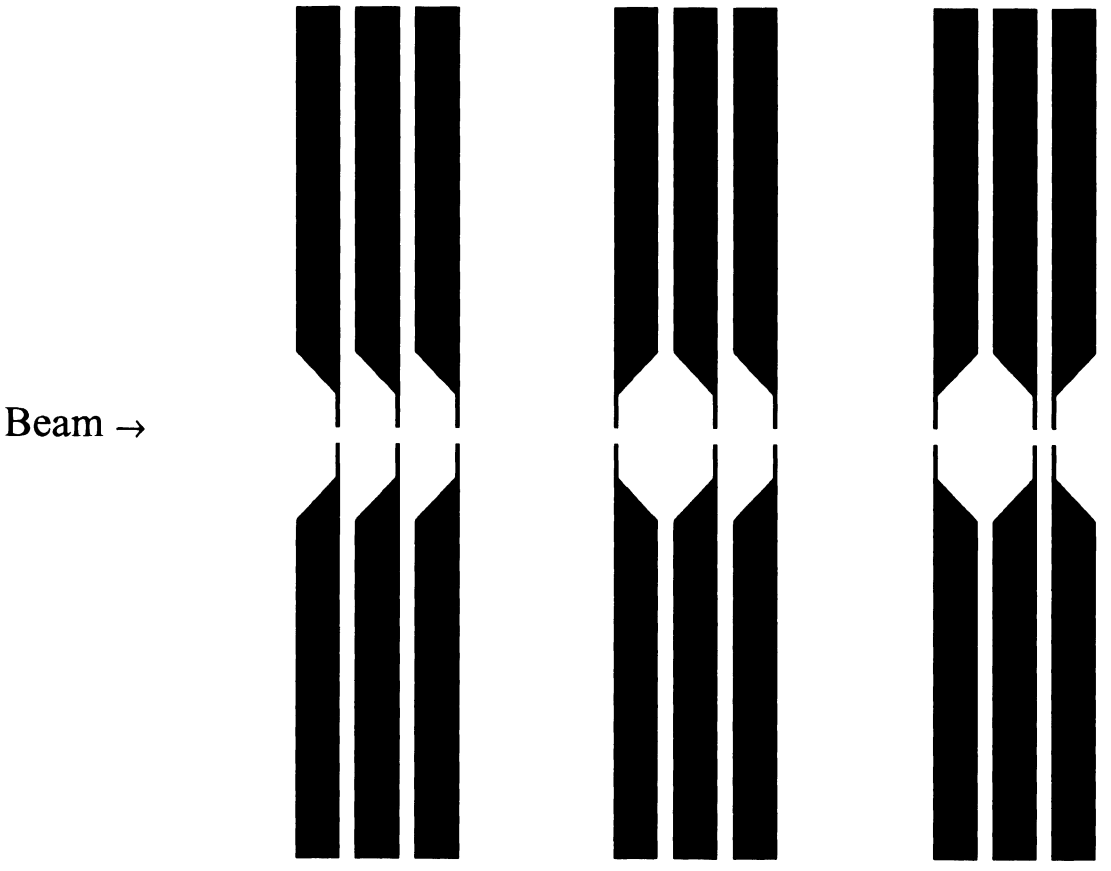

Figure 1.

Three possible lens designs using the MSEM construction method. The wafers are 380 microns thick and the insulating gap between the electrodes is 150 microns. The thickness of the dope-stopped diaphrams is 30 microns. The electrodes measure approximately 1 x1 cm. The source position is set in the calculations at 150 microns from the front surface of the first electrode, corresponding to an electron source integrated onto a silicon die with the proper v-groove pattern to be bonded to the first electrode.

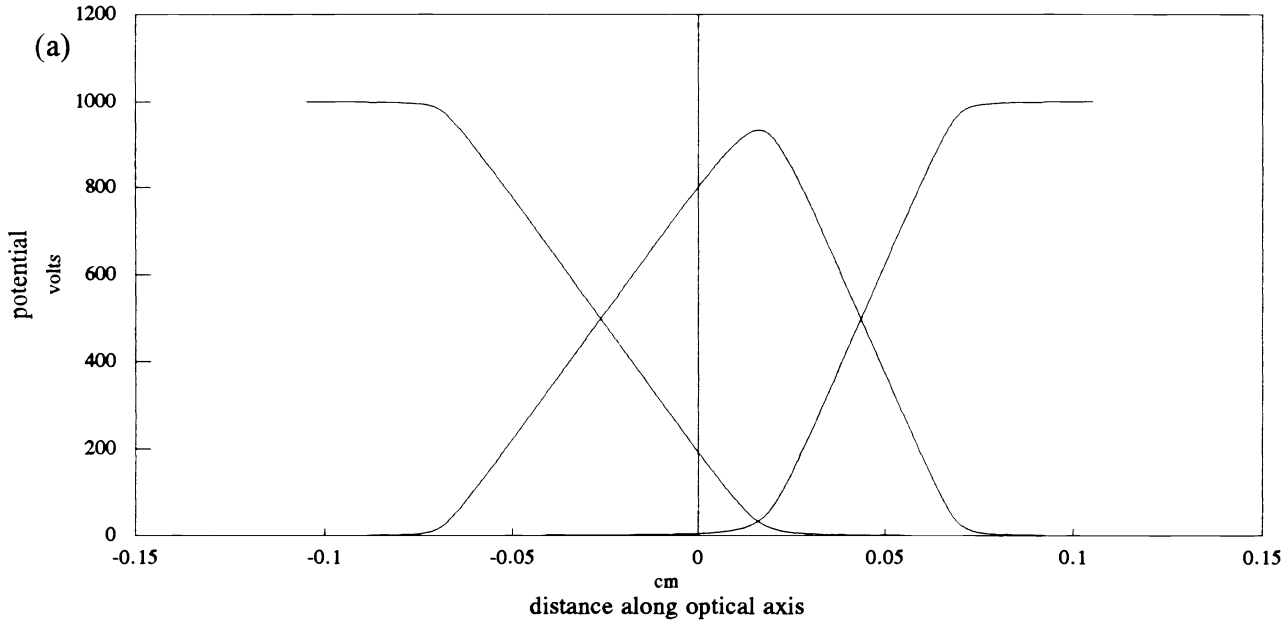

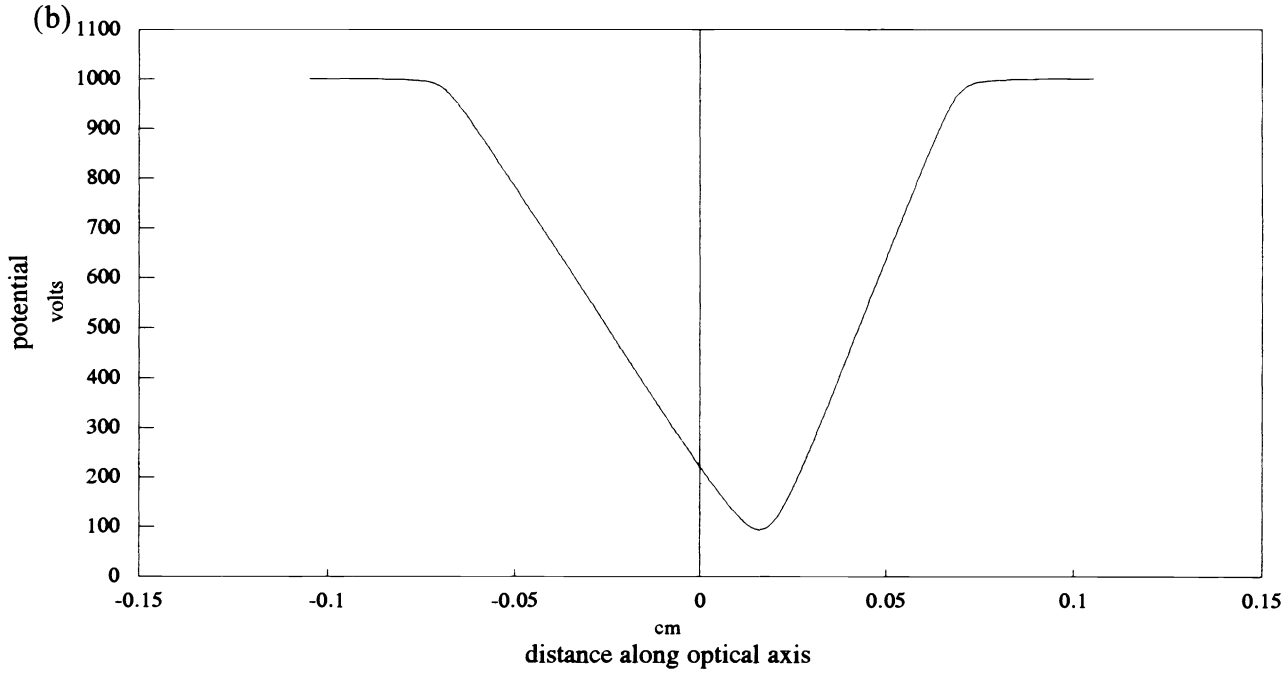

Figure 2

(a) Normalized axial potentials for the lens in figure 2(B). The three potentials are for each of the electrodes at 1000 volts and the other two at ground. The optical axis zero point is the physical center of the second (focusing) electrode. Note the second electrode potential does not reach 1000 volts, this is because the second electrode aperture (150 μm) is larger than the first and third (100 μm).

(b) A scaled superposition of the potentials in (a) with $V_1=V_3=$ 1 kv and $V_2=$150 volts.

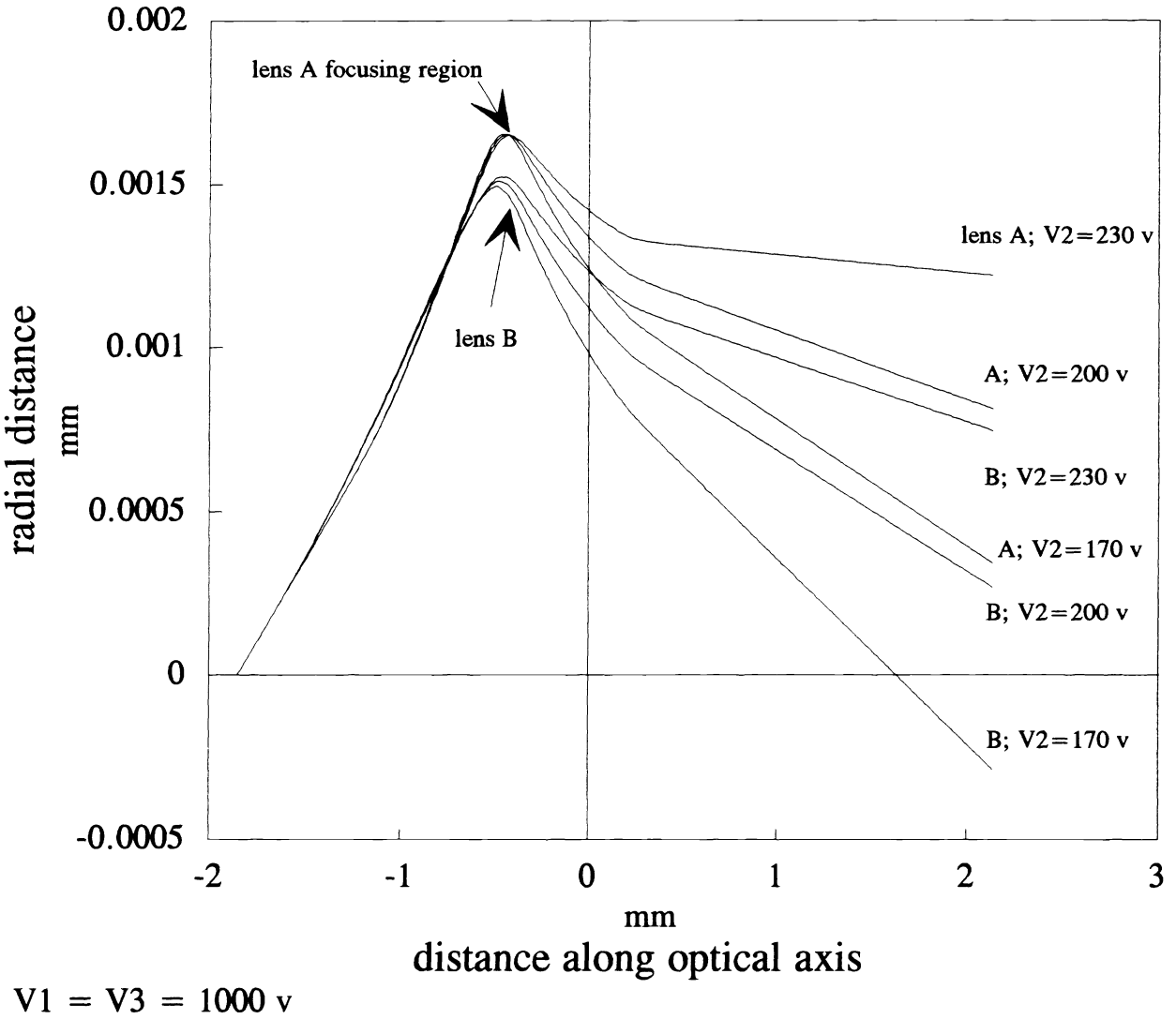

Figure 3

Several ray traces comparing the focusing effects of lenses A and B in figure 1. Lens B, with the aperture on the trailing edge of the die shows a later and more gradual focusing action. The initial conditions for the fourth order Runga-Kutta ray trace routine were a point source on axis 150 μm from the first electrode with an initial angle of 10 milliradians.

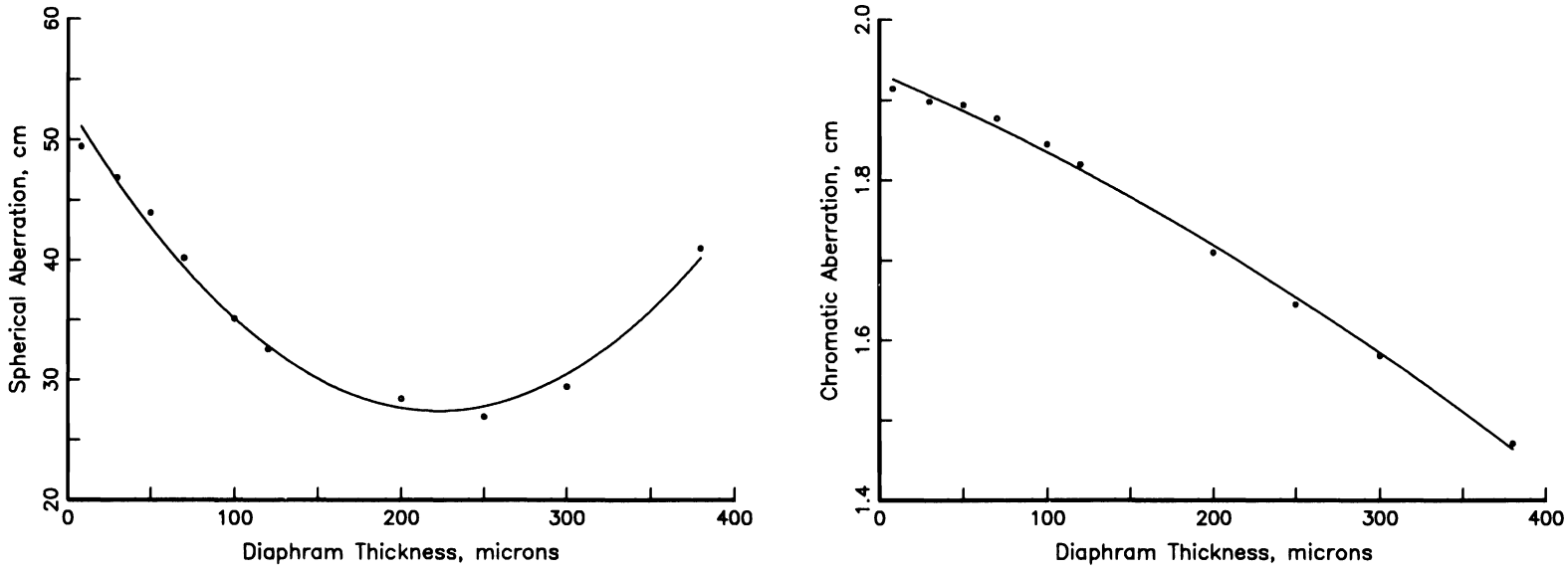

Figure 4

Cs and Cc vs the thickness of the diaphram containing the aperture on each electrode for a focus corresponding to a working distance of 0.5 mm. Spherical aberration reaches a minimum when the diaphragm is approximately one half the thickness of the electrode.

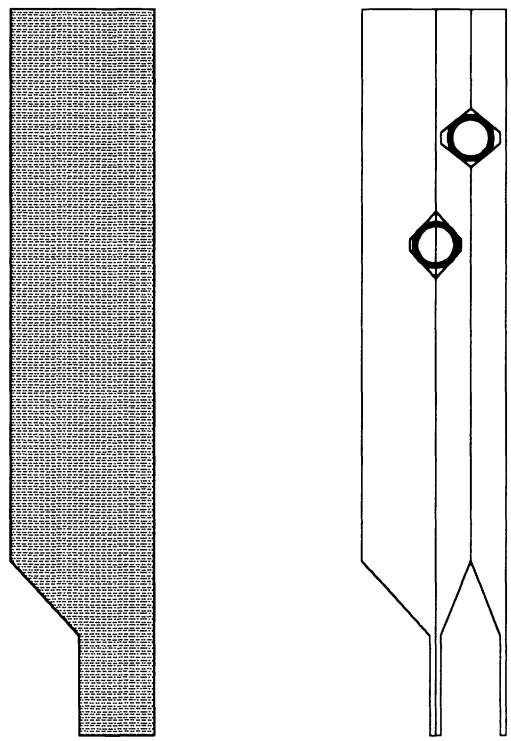

Figure 5

Very thick electrodes can be simulated by constructing electrodes out of three die placed back to back and bonded with zero gap between them. The zero gap alignment and anodic bonding would be done using microcapillary tubes metalized on the inside surface. The electrode to electrode alignment would then be done using the pyrex fiber technique.

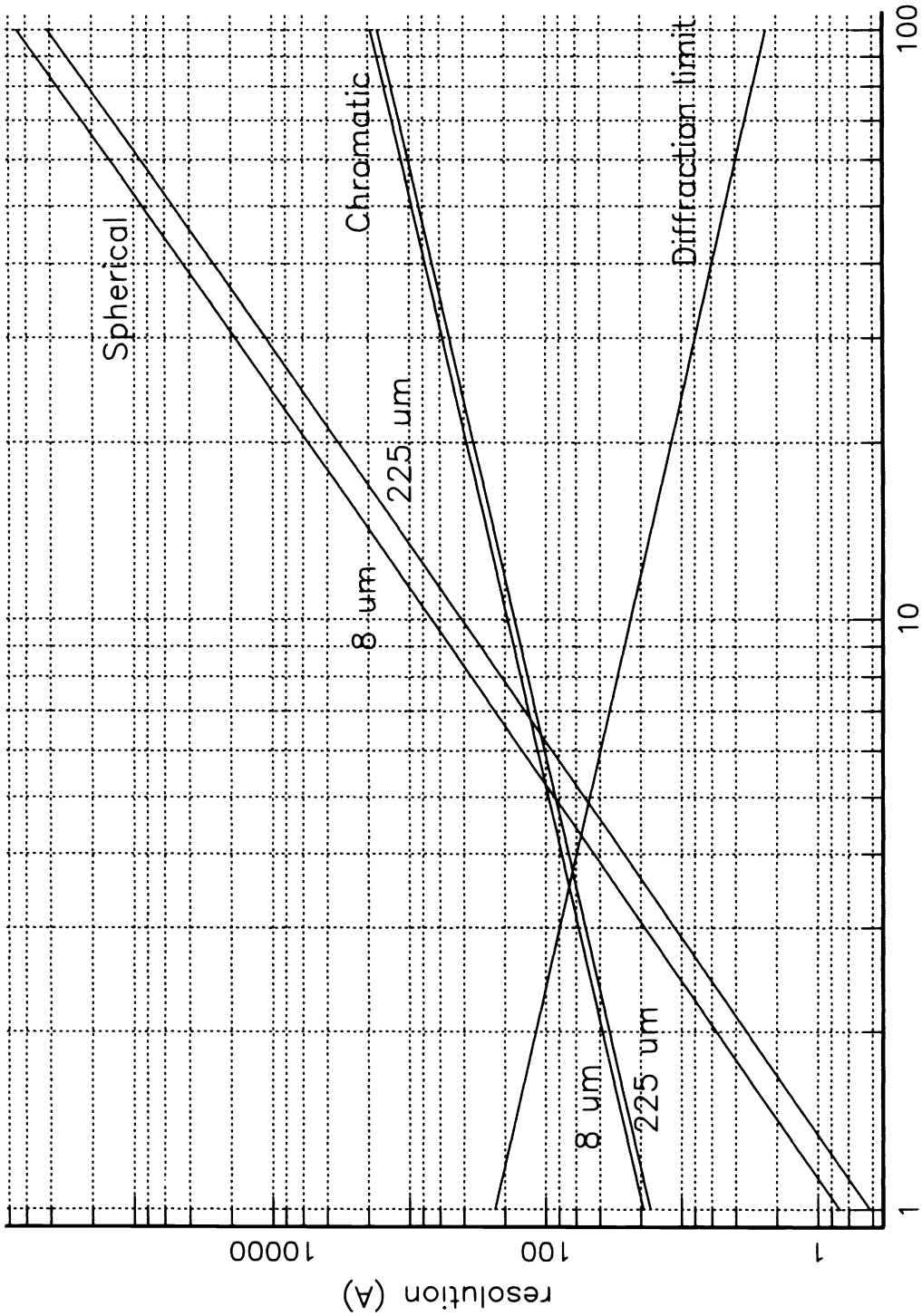

Figure 6

Resolution plots for two lenses of type (B) in figure 1. The lens with the lower effective C_s and C_c has diaphragms that are 225 microns thick, the slightly poorer performing lens has 8 micron thick diaphragms. The diffraction limit is the same for the two lenses, being dependent upon beam potential only. The expected resolution appears to be chromatic aberration limited and approximately 60 angstroms for the thick diaphragm lens and 70 angstroms for the thin diaphragm lens.